Remediation of textile industry organic dye waste by photocatalysis using eggshell impregnated ZnO/CuO nanocomposite

Mekdes Gerawork

ABSTRACT

Heterogeneous photocatalysis using nanocomposites is of great research interest in the treatment of industrial wastewater. The impregnated photocatalyst was produced by liquid state reaction of ZnO/CuO nanocomposite with extracted eggshells. The structure, functional group, metal composition, bandgap, and photocatalytic activity of the nanocomposites were characterized by using X-ray diffraction, Fourier-transform infrared spectroscopy, atomic absorption spectrometry, and UV–Vis spectroscopy, respectively, in the absence and presence of eggshells. Photocatalytic degradation activities of the nanocomposites under UV light irradiation have been tested for a real sewage sample taken from Debre Berhan Textile Industry. From the results, the optimized degradation efficiency of the dye was 97.95% with 0.4 g dose of the photocatalyst, 120 min irradiation time, 120 °C temperature, and pH of 6.7. The results revealed that eggshell impregnated nanocomposite had better catalytic activity than the naked nanocomposite. This is due to the highly porous structure of eggshell biomasses and their sorption characteristics. In conclusion, when nanocomposites are supported by eggshell biomasses, they are excellent photocatalysts and can minimize the contamination of organic dyes from textile effluents.

Key words | industrial waste, irradiation, nanocomposites, pH, photocatalysis

Mekdes Gerawork
Department of Chemistry, College of Natural and Computational Science,
Debre Berhan University,
P.O. Box 445 Debre Berhan,
Ethiopia
E-mail: *mgerawork2009@gmail.com*

HIGHLIGHTS

- Heterogeneous photocatalysis is a promising technology to remediate wastewater from industries.
- Eggshell supported nanocomposites are effective for degradation of textile dyes under UV irradiation.
- Waste eggshells can be recycled to support photocatalysts for wastewater treatment purposes.

INTRODUCTION

Textile dyeing industries consume a huge amount of water and they produce wastewater, which has a high content of organic dyes (Omprakash & Karthikeyan 2013). These organic dyes have defined colors that remain in the ground and are released into agricultural farms, which causes contamination of humans and agricultural systems (Mekdes 2020). Indeed, these dyes usually have a synthetic nature and a complex aromatic molecular structure, which makes them more stable and difficult to degrade. Thus, wastewater from these industries requires proper treatment before being released into the environment (Abdullah *et al.* 2019).

doi: 10.2166/wst.2021.165

It is therefore necessary to find an effective method for the treatment of such effluents. In recent years, heterogeneous photocatalysis using metal oxide nanocomposites is selective, which generates very reactive species such as hydroxyl radicals that oxidize a broad range of organic pollutants quickly and non-selectively (Mehali *et al.* 2014). Heterogeneous photocatalysis can be defined as the acceleration of a photoreaction in the presence of a catalyst. Moreover, it is inexpensive; can be carried out under ambient conditions; and does not produce secondary sludge for water pollution treatment (Neppolian *et al.* 2002; Rauf & Ashraf 2009). Among the various nanocomposites, the present study focused on ZnO/CuO due to its availability, non-toxicity, and economic benefits (Bruno *et al.* 2016). The economic advantage could be achieved by immobilizing the as-synthesized nanocomposite onto the support of biomasses, such as powdered eggshells. The main reason for choosing eggshell as support is because of their natural availability, low operating cost, minimal volume of secondary sludge to be disposed of, and it enhances the surface area of the composite's porous structure (Geetha & Belagali 2013).

The principal objective of this study was to design a functional ZnO/CuO nanocomposite, impregnated with eggshells by varying the parameters with the batch method. The properties of the nanocomposite were characterized by X-ray diffraction (XRD), Fourier-transform infrared spectroscopy (FTIR), atomic absorption spectrometry (AAS), and UV–Vis spectroscopies. Currently, Ethiopia is releasing wastewater containing organic dyes without proper treatment. These contaminants are carcinogenic and cannot be removed with conventional methods. Introducing such advanced technologies is mandatory for the complete treatment of the dyes. To this end, the photocatalytic activity of the nanocomposite was tested for the treatment of real methyl orange dye from textile industry effluent. The impregnated nanocomposite material had attractive efficiency of the dye compared to the investigation of Sharma *et al.* (2020) (96%). When we compared our results with the results of Naushad *et al.* (2019a) and Ali Shah *et al.* (2017) (75%), this study had better degradation efficiency of the dye. This is due to the presence of the porous structured eggshells support which enhances its degradation efficiency by delaying its agglomeration. This study demonstrated the attractive utilization of biomasses for the synthesis of such smart and environmentally friendly composite materials for photocatalytic applications.

MATERIALS AND METHODS

Chemicals, instruments, materials, and characterization

All the chemicals used in this study were analytically graded. For this research, the chemicals and reagents required were $CuSO_4.5H_2O$, KBr-pellet, HCl-37%, Methyl Orange, C_2H_5OH, distilled water, $Zn(NO_3)_{2.}6H_2O$, NaOH-pellet, KOH-1M, NaCl, and eggshells.

The structures of the nanocomposites were examined by powder XRD using X'Pert Pro PANalytical equipped with an X-ray source of a CuKα radiation (wavelength of 0.15406 nm) at a step scan rate of 0.02° (step time: 1 s; 2θ range: 5–80°). The particle size was calculated by Scherer's Equation (Ahmad *et al.* 2015):

$$D = \frac{K\lambda}{\beta \cos\theta} \tag{1}$$

where D is an average crystalline size in nm, K is 0.9, β is fullwidth at half max in rad of 2θ, λ is the wavelength of X-ray (0.15046 nm) for CuKα radiation, θ is the Bragg's angle. The functional group was determined by FTIR, band gaps of the nanocomposite using a UV–Vis absorption spectrophotometer (SP65), and the metal composition was detected by AAS. Finally, the bandgap energy of the nanocomposite (B_{eg}) can be determined using (Sher *et al.* 2013):

$$B_{eg} = \frac{1240}{\lambda}(\text{eV}) \tag{2}$$

Preparation of eggshell powder

The eggshells were washed with tap water to remove surface adsorption and then dried at 105 °C for 1 h in a convection oven, ground using a mortar and pestle then soaked with H_2SO_4 solution 1:1 weight (volume) overnight to increase adsorption efficiency. It was then washed with distilled water to reach a neutral pH and was treated 2% $NaHCO_3$ overnight to remove excess acid present. Then it was washed with distilled water to remove dirt, boiled to remove color, dried in an oven at 105 °C for 1 h, and activated in a furnace at 450 °C for 1 h. Finally, it was passed through 0.5–2 mm sieves. The powdered eggshell was then used in further experiments (Kassa & Akeza 2014).

Synthesis of the photocatalyst

The naked nanocomposite was prepared using a one-step precipitation method: from an aqueous solution of

$Zn(NO_3)_2.6H_2O$, ($CuSO_4.5H_2O$), and NaOH to precipitate the solution and heated at 80 °C, dried and calcined at 400 °C for 3 h (Siti *et al.* 2019). The eggshell supported photocatalyst was synthesized by mixing the extracted eggshell solution and the prepared photocatalyst, stirred, and, after solvent evaporation, the solid was dried and crushed to form a homogenous solid-state mixture. The powder was then be calcined at 300 °C for 1 h to get the impregnated photocatalyst (Li & Wang 2010; Kassa & Akeza 2014).

Photodegradation experiment

The photocatalytic activities of the prepared nanocomposites were examined by measuring the decomposition rate of methyl orange (MO). A 25 ppm dye solution sample was placed in front of the UV light source. The photocatalytic films were immersed in the solution, and the distance between the films and the lamp was kept at 5.0 cm using UV–Vis spectroscopy at λ_{max} of 464 nm. In a typical experiment, the reaction suspension was prepared by adding the desired photocatalyst load into a solution of the dye waste for 120 min, and samples were taken every 30 min, centrifuged, and filtered to remove the catalyst. Then the dye concentration was measured (Francisco *et al.* 2018) and the degradation efficiency (DE) calculated according to (Ahmad *et al.* 2015):

$$\%\mathrm{DE} = \frac{A_{0-A}}{A} \times 100 \tag{3}$$

where A_0 and A are the UV absorption of the original MO waste and MO after irradiation time, respectively.

Batch adsorption studies

Batch sorption studies were carried out with varying experimental conditions where all proportions were based on the capacity of the photocatalyst by referring to previous works for studying the effect of contact time (30–120 min), pH (3, 6.7, and 10), sorbent dose (0.1–1.2 g), and temperature (40, 80, and120 °C).

Effect of pH

The effect of pH on the adsorption of the waste solution onto the adsorbent was investigated by varying the pH of the solution from 3, 6.7, and 10. The parameters was adjusted to the desired pH level either with 0.1 M NaOH or 0.1 M HCl, by keeping all other parameters constant. Then 0.3 g of adsorbent was added to each solution and the degradation experiment repeated for each pH value.

Effect of contact time

To investigate the effect of contact time, experiments were conducted at initial dye waste concentration and the pH, adsorbent dose, and temperature were kept constant whilst varying the contact time to 30, 60, 90, and 120 min.

Effect of adsorbent dose

Photocatalyst dose was selected by varying the photocatalyst dose as 0.1, 0.2, 0.3, and 1.2 g whilst all other parameters (pH, contact time, and temperature) were kept constant.

Effect of temperature

To examine the effect of temperature, experiments were conducted by varying the temperature from 40, 80, and 120 °C and all other parameters (pH, adsorbent dose, contact time, and temperature) were kept constant.

RESULTS AND DISCUSSION

XRD analysis

The XRD spectra of naked and eggshell impregnated photocatalysts are shown in Figure 1.

From the results, ZnO peak intensities occurred at 2θ values of 31.8° (100), 34.4° (002), 36.3° (101), 47.5° (102), 56.5° (110), and 62.8° (022), while for CuO at 2θ values of 35.78° (002) and 39° (111). The structure of the naked ZnO/CuO composite sample was wurtzite hexagonal (JCPDS Card No. 36–1451) and monoclinic (JCPDS Card No. 05-661), which are in good agreement with the standard patterns of both oxides (Saravanakkumar *et al.* 2018). The same structure has been observed in impregnated nanocomposite (COD File No. 00-900-4179) for ZnO (Kihara & Donnay 1985) and CuO (COD File No. 00-901-6326) (Asbrink & Waskowska 1991), which are in agreement with the findings of Francisco *et al.* (2018). It can be suggested that when ZnO was coupled with CuO, their coupling inhibits the phase transformation (Fan *et al.* 2010). Trigonal $CaCO_3$ appeared according to (COD File No. 00-900-0095) and orthorhombic $CaSO_4$ (COD File No. 00-900-4096) (Hawthorne & Ferguson 1975). In both samples, their structure was identical. All samples had

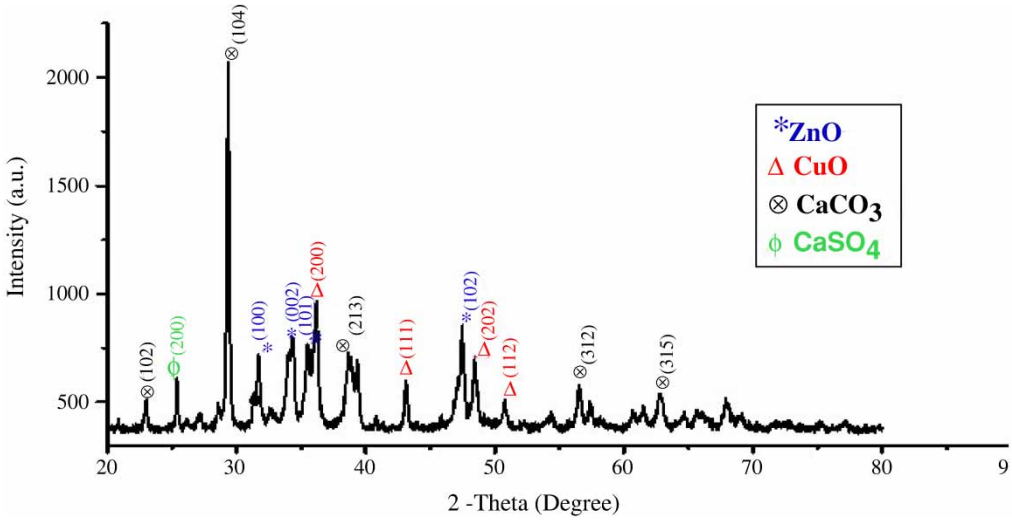

Figure 1 | XRD pattern of eggshell impregnated nanocomposite.

clear and intense peaks, which confirmed their purity and crystallinity (Saravanakkumar *et al.* 2018). Indeed, the peaks of $CaCO_3$ showed that a good proportion of the eggshells were impregnated. The particle size was 7.61 nm and 7.3 nm for the naked and the impregnated composite, respectively, which is a smaller size (15–16 nm) than the findings of Widiarti *et al.* (2017). This implies that the eggshell powder was providing biosorbents which increased the surface area by increasing the number of reaction sites on the nanocomposite (Widiarti *et al.* 2017; Mekdes 2020), thus improving photocatalytic activity.

FTIR analysis

Figure 2 shows FTIR spectra, which determines the functional groups of the nanocomposites. The wave numbers at 2,854.65 cm^{-1}, 2,922.59 cm^{-1}, and 2,931 cm^{-1} are C–H functional groups, and at 524 cm^{-1}, 594 cm^{-1} they are Cu–O bonds. The broad peak at 1,454 cm^{-} and 715 cm^{-1} could be Zn–O, which was similar to the findings of Widiarti *et al.* (2017). The O–H stretching vibration could be observed at 3,431 cm^{-} and stretching modes of C–O appeared at 1,110 cm^{-1}. The peak at 2,830 cm^{-1} is C–H stretching vibration of alkane groups. In fact, in the composite samples impregnated with eggshells, the wave numbers were observed at 871, 2,513, 1,413 cm^{-1}. Both Zn–O and Cu–O bands were recorded according to Widiarti *et al.* (2017). The O–H stretching vibration could be due to the water present at the surface of the nanocomposites. The stretching modes of C–O from the carbonate group also arise from the improper decomposition of eggshells (Abdullah *et al.*

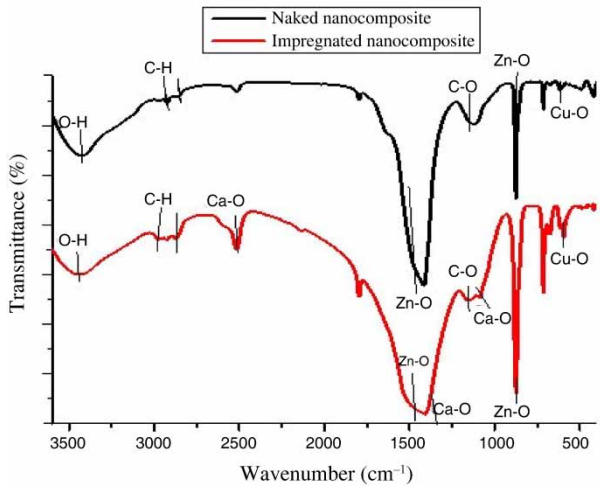

Figure 2 | FTIR spectrum of nanocomposite.

2019). The C–H stretching vibration was from alkane groups (Xiong *et al.* 2006). In the impregnated nanocomposite samples, the Ca–O and C–O bonds confirmed the presence of $CaCO_3$ during the impregnation process (Borhade & Kale 2017). From these FTIR results, the O–H bond was broader in the impregnated nanocomposite than the naked one due to the adsorption of more water from the surface of the metal oxides by the former composite. The intense peak of the Ca-O band confirmed the presence of more porous structured $CaCO_3$ in eggshells (Cu, Zn, and Ca) in the prepared photocatalysts (Xinghua & Da 2016). In general, the FTIR results confirmed the possible functional groups and the existence of eggshells that support photocatalytic activity.

In this experiment, the type of bond structure confirms the presence of the desired functional groups in the prepared photocatalysts.

AAS characterization

The amount of metals found in the naked and the impregnated nanocomposites were detected by the flame method using the AAS model NOVAA 400 with a detection limit of 10^{-4} mol/L. The results showed that only Cu, Zn, and Ca metals were detected, which confirms the presence of the targeted metals and purity of the prepared composites. Results showed that the average amounts of Cu and Zn in the naked composite was 20% and 80%, respectively. In the impregnated photocatalyst, the composition of Cu, Zn, and Ca metals were 12.11%, 78.48%, 74.98, respectively (Table 1). The atomic ratio was 0.25 and 0.15 in the naked and impregnated photocatalyst, which was far less than that of the raw materials (0.9) and is in good agreement with the standards (Xinghua & Da 2016). The smaller concentration of Cu confirms the incorporation of CuO into ZnO, and that Ca metal was present when the composite was impregnated with eggshells.

Table 1 | The atomic composition of Zn, Cu, and Ca

Type of sample	Zn (%)	Cu (%)	Ca (%)
ZnO/CuO composite	80	20	0
Eggshell impregnated ZnO/CuO composite	78.48	12.11	74.98

Batch adsorption experiment

Effect of catalyst load

The effect of catalyst load was tested from 0.1 g to 1.2 g and all other parameters were kept as constant as shown in Figure 3. From the results, it can be seen that as the dose of the naked photocatalyst increased from 0.1 g to 0.4 g, the removal efficiency increased from 79.61 to 85.45%, and for the impregnated from 88.92 to 94.97%. The optimized concentration was 0.4 g of the impregnated photocatalyst with efficiency (94.97%).

As the dose of the photocatalysts increased, the photodegradation efficiency of the photocatalysts also increased gradually. This is because the increase in catalyst increases the number of active sites on the photocatalyst surface, and thus causes an increase in the formation of the number of •OH radicals which can take part in actual discoloration of dye solution (Prabhu *et al.* 2019). Moreover, the photodegradation efficiency of the impregnated nanocomposite was more than the naked one. This might be because the microporous structure of eggshells increases the surface area, enhances the charge separation, and inhibits the recombination rate for better photocatalytic activity (Ahmad *et al.* 2015).

Effect of contact time

As shown in Figure 4, the effect of irradiation time was tested from 30 to 120 min when other parameters were kept constant. The degradation efficiency was increased from 90.2 to 90.4% and from 90.88 to 95.72% for the naked and the impregnated nanocomposite, respectively.

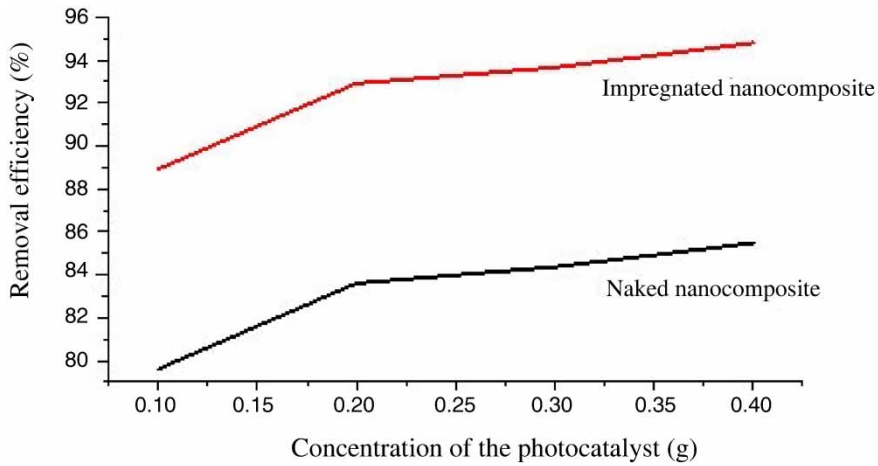

Figure 3 | Effect of concentration on photodegradation of MO dye.

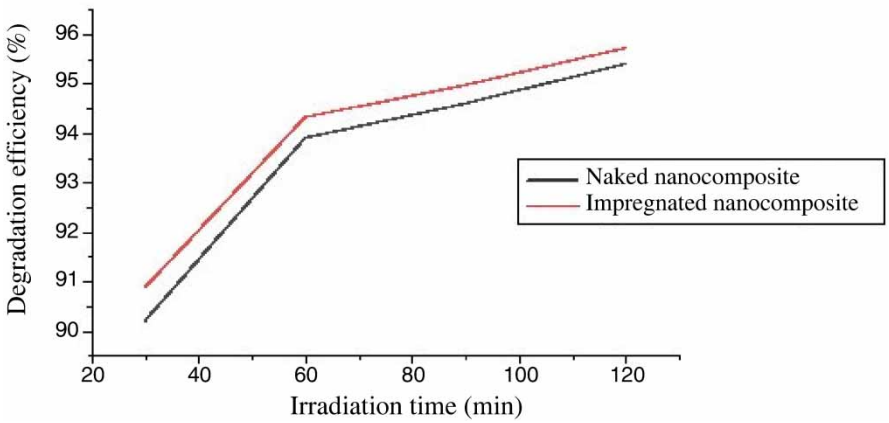

Figure 4 | Effect of irradiation time for degradation of MO for different exposure times.

The maximum removal efficiency was observed by the impregnated photocatalyst with an efficiency of 95.72% at 120 min. This is due to the delayed electron-hole recombinations resulting from the introduction of extra bands as the result of the impregnation of porous eggshells to the naked nanocomposite (Fan *et al.* 2010).

Effect of pH

As shown in Figure 5, the removal of the dye was significantly affected by the pH of the solution. The rate of catalytic reactions can be shifted with the variation of pH by changing the net charge of the nanocomposite as well as the pollutant (Azad & Gajanan 2017). First, the $pH_{initial}$ against pH_{final} of the photocatalyst in 0.1 M NaCl were compared. In this range, the pH_{final} is almost the same for all values of $pH_{initial}$ and corresponds to pH_{pzc}. The pH_{pzc} of the catalyst was observed to be pH 8. Thus, the catalyst had a net positive surface charge at $pH < pH_{pzc}$ and a negative surface charge at $pH > pH_{pzc}$. (Naushad *et al.* 2019b). As the pH increased from 3 to 6.7, the degradation efficiency of MO increased from 93.85 to 95.34% and then decreased to 94.5% for the naked photocatalyst. For the impregnated photocatalyst, it increased from 94.51 to 97.95% and then decreased to 95.44%. The optimum degradation efficiency was 97.95% for the eggshell-supported catalyst at pH 6.7. This is because the photocatalyst is positively charged at lower pH, the number of negatively charged sites on the adsorbent surface decreases, and the number of positively charged sites increases, leading to an increase in the negatively charged dye removal (Fahim *et al.* 2013). Similar findings were reported by Prabhu *et al.* (2019).

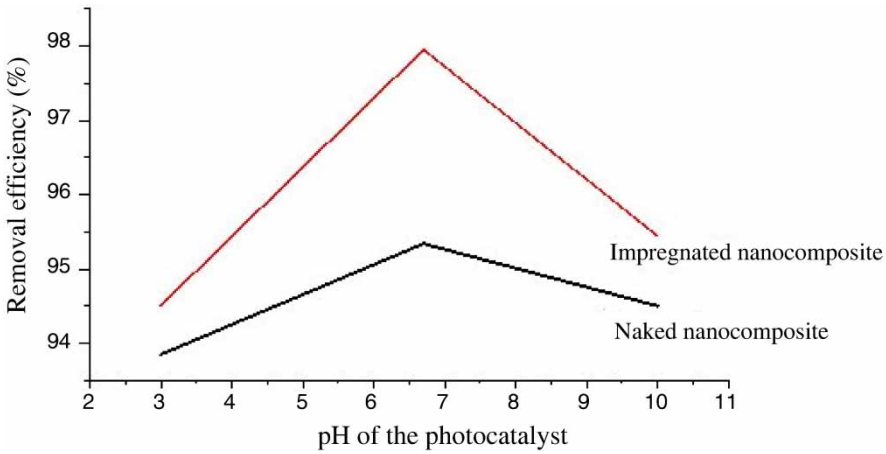

Figure 5 | Effect of pH.

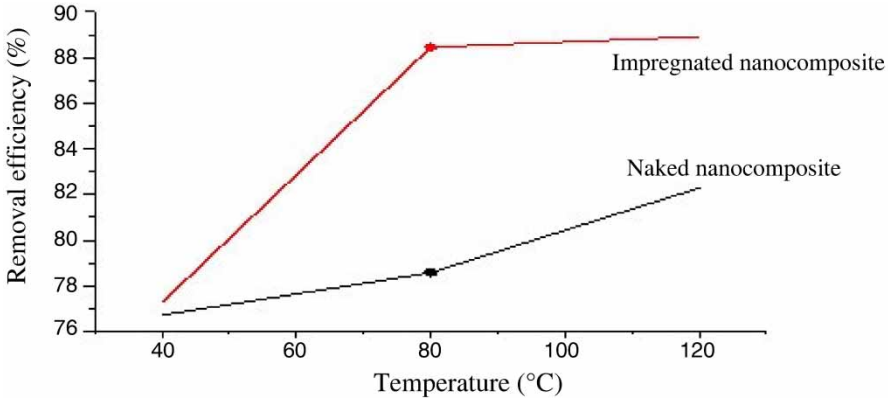

Figure 6 | Effect of temperature.

Effect of temperature

The photocatalytic activity of the prepared nanocomposite was tested at a temperature of 40 °C intervals (40–120 °C), as shown in Figure 6. The results revealed that, as the temperature increased, the removal efficiency also increased from 76.72 to 82.3% and from 77.28 to 88.92% for the naked and impregnated nanocomposite, respectively. As the temperature increased more dye molecules were adsorbed, with the optimum removal efficiency of 88.92% at 120 °C. This is because as the temperature increases the reactions involving electron-hole formation are predominant and electron-hole recombination is negligible for the increment of the rate of the reaction (Azad & Gajanan 2017).

This suggets that the adsorption of MO dye on the photocatalyst was an endothermic process (Naushad *et al.* 2019b)

Optical properties

To study the optical properties of the composite and absorption spectra of MO waste, the UV–Vis spectrum was recorded, as shown in Figure 7, under UV irradiation. The band gaps energy of the naked and impregnated nanocomposite were 2.6 and 2.5 eV, respectively. The redshift in the optical property of the impregnated nanocomposite compared with the naked one confirms that the use of eggshells can narrow the bandgap energy and allow the light absorption to be widened into the visible region for

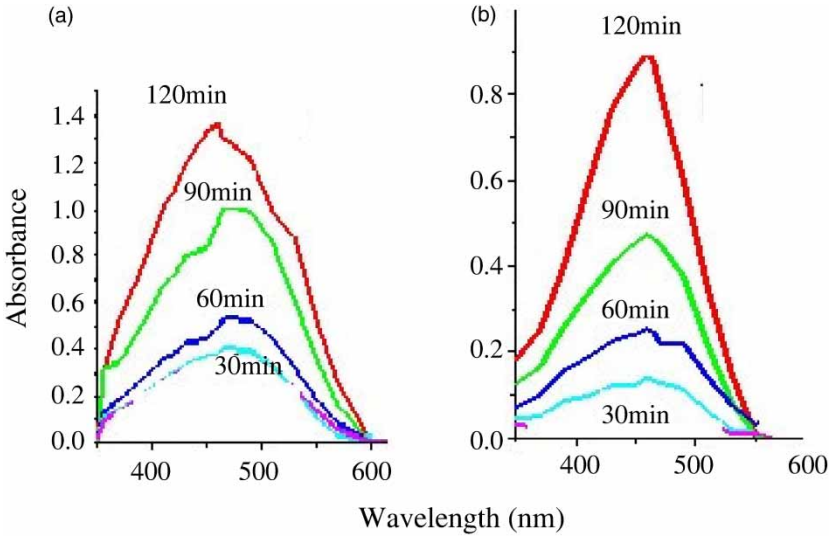

Figure 7 | UV-Vis spectra of photocatalysts (a) naked (b) impregnated nanocomposite.

better photocatalytic activity (Azad & Gajanan 2017). The results were in good agreement with the findings of Abdullah *et al.* (2019).

CONCLUSION

From the simple synthesis method, highly crystalline eggshell impregnated ZnO/CuO nanocomposite was synthesized. The results have shown that eggshell impregnated ZnO/CuO nanocomposites possess higher photocatalytic degradation of MO compared to the naked composite under UV light. The optimum removal of MO dye by impregnated nanocomposite was 97.95%. The maximum degradation efficiency was observed with 0.4 g of the photocatalyst, 120 min of contact time, at 120 °C, and pH 6.7. Color removal of dyes occurred due to the adsorption of dye molecules onto nanocomposite, therefore the adsorption of dye on eggshell-impregnated ZnO/CuO increased with the increase in concentration, contact time, and temperature, while it decreased with an increase of pH.

In all experiments the optoelectronic and photodegradation efficiency of the impregnated samples confirms the positive effect of supporting nanocomposites with such biomasses. In conclusion, supported nanocomposites can enhance the active sites on the nanocomposite for photocatalysis, and thus can be used to reduce contamination from wastewater.

ACKNOWLEDGEMENTS

I am very grateful to Debre Berhan University for its financial support and Addis Ababa University is duly acknowledged for the facilitation of their laboratory.

DECLARATION OF COMPETING INTEREST

There is no conflict of interest to declare.

DATA AVAILABILITY STATEMENT

Data cannot be made publicly available; readers should contact the corresponding author for details.

REFERENCES

Abdullah, A. M. S., Shah, M. M., Jan, H., Rafiqul, I. & Md, A. I. M. 2019 Synthesis of CuO/ZnO nanocomposites and their application in photodegradation of toxic textile dye. *Journal of Composites Science* **3**, 91.

Ahmad, R. Y., Gharib, M., Mehdi, T. R., Mohsen, A., Shahram, N., Meysam, E., Kale, S. M. & Maryam, S. T. 2015 Using eggshell in acid orange 2 dye removal from aqueous solution. *Iranian Journal of Health Sciences* **3** (2), 38–45.

Ali Shah, L., Sayed, M., Fayaz, M., Bibi, I., Nawaz, M. & Siddiq, M. 2017 Ag-loaded thermo-sensitive composite microgels for enhanced catalytic reduction of methylene blue. *Nanotechnology for Environmental Engineering* **2** (14), 1–7.

Asbrink, S. & Waskowska, A. 1991 CuO: X-ray single-crystal structure determination at 196 K and room temperature. *Journal of Physics: Condensed Matter* **3**, 8173–8180.

Azad, K. & Gajanan, P. 2017 A review on the factors affecting the photocatalytic degradation of hazardous materials. *Material Science & Engineering International Journal* **1** (3), 106–114.

Borhade, A. V. & Kale, A. S. 2017 Calcined eggshell as a cost-effective material for removal of dyes from aqueous solution. *Appl Water Science* **7**, 4255–4268.

Bruno, L., Chandrasekar, C. R., Karunakaran, M. & Vijayalakshmi, R. 2016 Synthesis and characterization of copper oxide and zinc oxide nanomaterials. *Nature of Scientific Materials* **1**, 18–22.

Fahim, B., Abdurrahman, M. A. & Abedin, M. Z. 2013 Dyes removal from textile wastewater using orange peels. *International Journal of Scientific & Technology Research* **2** (9), 48–50.

Fan, T., Han, T., Chow, S. K. & Zhang, D. 2010 Biogenic N–P-codoped TiO_2: synthesis, characterization and photocatalytic properties. *Bioresource Technology* **101**, 6829–6835.

Francisco, A. C., Gustavo, C., Ana, B. & Ricardo, S. S. 2018 Synthesis and characterization of a ZnO/CuO/Ag composite and its application as a photocatalyst for methyl orange degradation. *International Journal of Electrochemical Science* **13**, 9242–9256.

Geetha, K. S. & Belagali, S. L. 2013 Removal of heavy metals and dyes using low-cost adsorbents from aqueous medium: A review. *Journal of Environmental Science, Toxicology and Food Technology* **4**, 56–68.

Hawthorne, F. C. & Ferguson, R. B. 1975 Anhydrous sulphates II. Refinement of the crystal structure of anhydrite. *The Canadian Mineralogist* **13**, 289–292.

Kassa, B. & Akeza, H. H. 2014 Removal of Methyl Orange from aqueous solutions using thermally treated egg shell (locally available and low cost biosorbent). *Chemistry and Materials Research* **6**, 31–33.

Kihara, K. & Donnay, G. 1985 Anharmonic thermal vibrations in ZnO model. *The Canadian Mineralogist* **23**, 647–654.

Li, B. & Wang, Y. 2010 Facile synthesis and photocatalytic activity of ZnO-CuO nanocomposite. *Superlattices and Microstructures* **47**, 615–623.

Mehali, J., Mehta, K. & Chorawala, K. 2014 Adsorptive removal of dye from industrial dye effluents using low-cost adsorbents: a review. *International Journal of Engineering Research and Applications* **4** (12), 40–44.

Mekdes, G. 2020 Photodegradation of methyl orange dye by using zinc oxide–copper oxide nanocomposite. *International Journal for Light and Electron Optics* **216**, 1–6.

Naushad, M., Sharma, G. & Alothman, Z. A. 2019a Photodegradation of toxic dye using Gum Arabic-crosslinked poly (crylamide)/$Ni(OH)_2$/FeOOH nanocomposites hydrogel. *Journal of Cleaner Production* **241**, 118263.

Naushad, M., Abdullah Alqadami, A., Abdullah AlOthman, Z., Hotan A, I., Algamdi, M. S. & Mohammed Aldawsari, A. 2019b Adsorption kinetics, isotherm and reusability studies for the removal of cationic dye from aqueous medium using arginine modified activated carbon. *Journal of Molecular Liquids* **293**, 111442.

Neppolian, B., Choi, H. C., Sakthivel, S. A. B. & Murugesan, V. 2002 Solar light induced & TiO_2 assisted degradation of textile dye reactive blue 4. *Chemosphere* **46**, 11–73.

Omprakash, S. & Karthikeyan, M. R. 2013 Reduction of textile dyes by using heterogeneous Photocatalysis. *American Journal of Environmental Protection* **2** (3), 90–94.

Prabhu, S., Megala, S., Harish, M., Navaneethan, P., Maadeswaran, S. & Sohila, S. 2019 Enhanced photocatalytic activities of ZnO dumbbell/reduced graphene oxide nanocomposites for degradation of organic pollutants via efficient charge separation pathway. *Applied Surface Science* **487**, 1279–1288.

Rauf, M. A. & Ashraf, S. S. 2009 Application of Advanced oxidation Processes (AOP) to dye degradation – an overview. In: *Dyes and Pigments: New Research* (A. R. Lang, ed.). Nova Science Publishers, Inc, New York.

Saravanakkumar, D., Sivaranjani, S., Kaviyarasu, K., Ayeshamariam, B., Ravikumar, S., Pandiarajan, C., Veeralakshmi, M. & Jayachandranand, M. M. 2018 Synthesis & characterization of ZnO/CuO nanocomposites powder by modified perfume spray pyrolysis method and its antimicrobial investigation. *Journal of Semiconductor* **39** (3), 1–8.

Sharma, G., Kumar, A., Sharma, S., Naushad, M., Dhiman, P., D.Viet, N., Florian, V. & Stadler, J. 2020 Fe_3O_4/ZnO/Si_3N_4 nanocomposite based photocatalyst for the degradation of dyes from aqueous solution. *Journal of Materials Letters* **278**, 128359.

Sher, B. K., Faisal, M., Mohammed, M., Rahman, K. A., Abdullah, M., Anish, K. & Khalid, A. 2013 Alamry effect of particle size on the photocatalytic activity and sensing properties of CeO_2 nanoparticles. *International Journal of Electrochemical Science* **8**, 7284–7297.

Siti, N. S., Abdul, H. A. & Ernee, N. M. 2019 Response surface methodology: photodegradation of methyl orange by CuO/ZnO under UV light irradiation. *Asian Journal of Green Chemistry* **3**, 271–287.

Widiarti, N., Sae, J. K. & Wahyuni, S. 2017 Synthesis CuO – ZnO nanocomposite and its application as an antibacterial agent. *Materials Science and Engineering* **172**, 1–12.

Xinghua, M. & Da, D. 2016 Trash to treasure: waste eggshells used as reactor and template for synthesis of Co_9S_8 nanorod arrays on carbon fibers for energy storage. *Chemistry of Materials* **28**, 3897–3904.

Xiong, G., Pal, U., Serrano, J. G. K., Ucer, B. & Williams, R. T. 2006 Photoluminescence and FTIR study of ZnO nanoparticles: the impurity and defect perspective. *Physica Status Solid* **3** (10), 3577–3581.

First received 13 March 2021; accepted in revised form 15 April 2021. Available online 29 April 2021